Research Square

Preprints are preliminary reports that have not undergone peer review.
They should not be considered conclusive, used to inform clinical practice,
or referenced by the media as validated information.

Screening of benzoic acid degrading bacteria and their alleviating effects on tomato autotoxicity

Jianmei Che

chejm2002@163.com

Fujian Academy of Agricultural Sciences

Miaomiao Liu
Junhao Huang
Xuefang Zheng
Jieping Wang
Yanping Chen
Dongliang Qiu

Research Article

Keywords: Continuous cropping obstacle, benzoic acid, degrading bacteria, Bacillus, tomato

Posted Date: November 17th, 2026

DOI: https://doi.org/10.21203/rs.3.rs-11601146/v1

License: This work is licensed under a Creative Commons Attribution 4.0 International License.
Read Full License

Title: Screening of benzoic acid degrading bacteria and their alleviating effects on tomato autotoxicity

Authors: Miaomiao Liu[1], Junhao Huang[1], Xuefang Zheng[2], Jieping Wang[2], Yanping Chen[2], Dongliang Qiu[1*], Jianmei Che[2*]

Affiliation: 1. College of Horticulture, Fujian Agriculture and Forestry University, Fuzhou 350002, China

2. Institute of Resources, Environment and Soil Fertilizer, Fujian Academy of Agricultural Sciences Fuzhou, Fujian, People's Republic of China.

Corresponding author: Prof. Dr. Che Jianmei

Institute of Resources, Environment and Soil Fertilizer, Fujian Academy of Agricultural Sciences Fuzhou, Fujian, People's Republic of China.

Pro. Dr. Qiu Dongliang

College of Horticulture, Fujian Agriculture and Forestry University, Fuzhou, Fujian, People's Republic of China.

Abstract: The autotoxicity stress resulting from the accumulation of benzoic acid significantly restricts the sustainable development of facility tomatoes. In this study, two high-efficiency benzoic acid-degrading strains, *Peribacillus frigoritolerans* FJAT-49528 and *Peribacillus simplex* FJAT-53808, were screened. Both of these strains can effectively degrade benzoic acid and exhibited broad-spectrum degradation capabilities for various phenolic acid autotoxic substances. Additionally, both strains exhibited plant growth-promoting functions, including IAA production, organic phosphorus solubilization, and siderophore production. Whole-genome analysis and annotation identified key genes involved in multiple phenolic acid degradation pathways in the two strains. These genes are involved in the catabolism of various phenolic acid substrates such as benzoic acid, protocatechuic acid and 4-hydroxybenzoic acid. Potted experiments showed that the two *Bacillus* strains significantly alleviated benzoic acid-induced stress in tomato plants. On the 10th day under benzoic acid stress, compared with the control group, the POD activity in the benzoic acid group decreased by 74.48%, while the T1 and T2 treatment groups showed increases of 13.38% and 11.30% respectively. The PPO activity in the T1 group reached 401.33 U/g at the same time, which was 36.2% higher than the benzoic acid group. By day 30, the MDA content in the T1 and T2 groups was reduced by 16.5% and 13.6% respectively compared to the control group, effectively suppressing membrane lipid peroxidation damage. Overall, these findings show that *Peribacillus frigoritolerans* FJAT-49528 and *Peribacillus simplex* FJAT-53808 are potential benzoic acid-degrading strains in continuous cropping application.

Keywords: Continuous cropping obstacle; benzoic acid; degrading bacteria; *Bacillus*; tomato

1. Introduction

The obstacle of continuous cropping poses a significant constraint to the sustainable development of facility agriculture. Prolonged reliance on monoculture leads to the degradation of soil physicochemical properties, microbial community imbalance, and accumulation of autotoxic substances, all of which severely inhibit crop growth and yield(Li et al. 2024a). The key underlying factors include the accumulation of soil-borne pathogens and the persistent release of phenolic acids. Among these, benzoic acid (BA), a typical phenolic acid allelochemical, accumulates progressively in soil under long-term continuous tomato cropping. It not only directly inhibits seed germination and root growth but also induces oxidative stress by disrupting cell membrane lipid peroxidation and triggering the production of reactive oxygen species (ROS). Furthermore, it modifies the rhizosphere microbial community structure, thereby increasing the susceptibility to soil-borne disease such as bacterial wilt(Li et al. 2024c). Therefore, the development of efficient and environmentally friendly methods to degrade benzoic acid in soil and mitigate its toxic effects has become a critical challenge in overcoming the problems linked to continuous tomato cropping.

Current strategies to mitigate phenolic acid accumulation include soil management, chemical treatments, biochar adsorption, combined application of biochar with chemical oxidants, and microbial degradation(Jiang et al. 2022). However, due to factors such as high costs and environmental impact, these strategies are not suitable for wide implementation. In contrast, biodegradation harnesses the metabolic capabilities of microorganisms to mineralize or transform phenolic acids, providing benefits such as environmental compatibility, cost-effectivenes, and strong sustainability. Therefore, it is considered the most promising treatment approach(Huang et al. 2018; Esikova et al. 2021; Hu et al. 2024). Numerous microorganisms capable of degrading benzoic acid have been isolated from diverse habitats(Li et al. 2017; Aromokeye et al. 2021; Esikova et al. 2021; Emelyanova et al. 2023). *Pseudomonas* sp. QTF5, isolated from the permafrost region of the Qinghai-Tibet Plateau, not only metabolizes benzoic acid but also exhibits tolerance to multiple stresses, including low temperatures and heavy metals(Li et al. 2017). In recent years, *Bacillus* has garnered significant attention due to its unique metabolic potential and growth-promoting characteristics(Liu et al. 2024). *Bacillus thuringiensis* B1, *Bacillus amyloliquefaciens* B2 and *Bacillus subtilis* B3 exhibited significant phenolic acid degradation abilities. These strains effectively degrade a variety of representative phenolic acids, including ferulic acid, ρ-coumaric acid, ρ-hydroxybenzoic acid (PHBA), and cinnamic acid, thereby significantly alleviating the inhibitory effects of these phenolic acids on peanut seed germination and growth(Zhang et al. 2024b). *Bacillus licheniformis* TAB7 is capable of effectively biotransforming various monocyclic phenolic compounds, including ferulic acid, vanillic acid, and ρ-coumarate, within a complex composting environment(Mpofu et al. 2019). These studies directly demonstrate the key role of *Bacillus* in mitigating plant autotoxicity. Additionally, *Bacillus* strains have demonstrated tolerance to a variety of stress factors. For instance, an alkali-resistant and heat-resistant strain *Bacillus halootolerans* ACY in alkaline high-load wastewater, when combined with biochar immobilization technology, can increase the removal rate of phenolic substances in actual phenolic wastewater to 99.5% within 7 days. Its efficiency is significantly higher than that of biochar or free bacteria used individually(An et al. 2024), highlighting the the substantial application potential of *Bacillus* in the remediation of highly polluted environments. However, there are still relatively few related screenings conducted at present.

Genome analysis has provided crucial insights into the molecular mechanisms underlying the microbial degradation of aromatic compounds. The genome analysis of *B. licheniformis* TAB7 revealed that this strain carries genes associated with phenolic acid decarboxylase, vanillic acid decarboxylase, and protocatechuate degradation pathways(Mpofu et al. 2019). A combined whole-genome and transcriptome analysis of KLS-1 uncovered its complete metabolic pathway for degrading vanillic acid into β-ketoadipate via vanillic acid decarboxylase and the ortho-cleavage pathway of protocatechuate(Han et al. 2024). These studies demonstrate that genome analysis has become a powerful tool for elucidating the potential of microbial strains to degrade aromatic compounds. In this study, two *Bacillus* strains exhibiting high-efficiency degradation of benzoic acid were isolated. Their growth characteristics were studied, functional genes were analyzed, and effects on tomato growth and enzyme activities were observed. Our findings will lay a foundation for investigating the mechanisms by which degrading bacteria degrade phenolic acids and will provide a theoretical basis for the application of phenolic acid-degrading *Bacillus* in the bioremediation of soils affected by continuous cropping obstacles.

2. Materials and Methods

2.1 Strains and their sources

All the strains used in this study were isolated from the grape root in Fuan, Fujian Province, PR China.

2.2 Screening of degrading bacteria

Single colonies were selected and transferred to benzoic acid solid medium, where several strains exhibiting robust growth were initially screened. Subsequently, these selected strains were inoculated into LB liquid medium under cultivation conditions of 30 °C and 180 rpm for 24 hours. Following this, the strains were transferred to a liquid medium containing 0.5 g/L benzoic acid at a volume ratio of 2%. After three days, the absorbance of the fermentation broth was measured at a wavelength of 230 nm using ultraviolet spectroscopy to determine the residual concentration of benzoic acid. This enabled the evaluation of each strain's degradation capacity for benzoic acid, resulting in the identification of the strain with the highest degradation ability(Zhang et al. 2024a).

2.3 Degradation effect of benzoic acid by different strains

Determination of the benzoic acid standard curve: A series of benzoic acid standard solutions with concentrations of 2.5, 5, 7.5, 10, 15, 20, 30, 40, and 60 mg/L were prepared. The blank medium served as a reference. Each concentration was measured in triplicate, and the absorbance was recorded at 230 nm. The concentration of benzoic acid was plotted on the x-axis, while the absorbance was plotted on the y-axis. The standard curve was generated using Excel software, followed by linear fitting.

Determination of the degradation ability: The strains were inoculated into LB liquid medium and incubated for 24 hours at 180 r/min and 30 °C to prepare the seed culture. For the experimental group, the seed culture was subjected to 4 °C and 8000 r/min for 5 minutes, after which the supernatant was discarded. The bacterial pellet was resuspended in sterile water to achieve an optical density (OD_{600}) of 0.8. A volume ratio of 2% of this suspension was inoculated into a basic medium containing benzoic acid at initial concentrations of 0.1, 0.5, 1, 1.5, and 2 g/L. The control group was not inoculated with bacteria and received the same volume of sterile water, with all other conditions remaining consistent with the experimental group. After inoculation, the cells were cultured at 30 °C and 180 r/min for 3 days. Samples were collected and centrifuged at 8000 r/min for 10 minutes. The absorbance at the maximum absorption peak wavelength was determined using ultraviolet-visible spectrophotometry. The degradation rate was calculated as follows: (control absorbance - treated sample absorbance) / control absorbance × 100%(Liu et al. 2025)

Assay of degradation spectrum: The strains were inoculated into MSM medium containing salicylic acid, PHBA, cinnamic acid, and ferulic acid as substrates (0.5 g/L) at 30 °C and 180 r/min for 3 days. Samples were collected after 3 days of shaking culture, following the aforementioned method for assessing degradation ability. The degradation rate of each phenolic acid in the culture medium was calculated based on the standard curve for each phenolic acid.

2.4 Identification of different strains

Single colonies of the screened strains were streaked on LB solid medium and cultured at 30 °C for 24 hours. The colony morphology and color were initially observed, followed by microscopic examination and transmission electron microscopy of the bacteria.

The genomic DNA of the strain was extracted in accordance with the instructions provided by the bacterial genomic DNA extraction kit. Subsequently, PCR amplification was performed. Upon completion of the PCR, the product was loaded onto an agarose gel for electrophoresis and visualized using a gel imaging system. The PCR products were then sequenced, and the obtained sequences were homologously aligned using BLAST in NCBI to construct a phylogenetic tree.

2.5 Growth characteristics of different strains

Preparation of bacterial suspension: Each strain was inoculated onto LB solid medium and cultured at 30 °C for 24 hours. Single colonies were then selected and inoculated into LB liquid medium, where they were cultured at 30 °C with shaking at 180 r/min for an additional 24 hours. The OD_{600} value of the bacterial suspension was adjusted to 1.0 (approximately 10^8 CFU/mL) to prepare the seed liquid.

Determination of the growth curve: Seed cultures were inoculated into LB medium at an inoculation ratio of 1% (v/v) and cultured at 30 °C under shaking conditions at 180 r/min. Culture aliquots were harvested at 0, 2, 4, 6, 8, 10, 24, 26, 28, and 30 hours, and the OD_{600} value of each aliquot was measured spectrophotometrically.

The effect of temperature on the growth of the strain: The seed liquid was inoculated in LB medium at temperatures of 10 °C, 20 °C, 30 °C, 40 °C, and 50 °C with a volume ratio of 1%. The cultures were agitated at 180 r/min for 24 hours,

and the absorbance at 600 nm was measured. To assess the effect of pH on the degradation of phenolic acids, LB medium was prepared and the pH was adjusted to 1.0, 3.0, 5.0, 7.0, 9.0, and 11.0 using 6M NaOH or 6M HCl. Following inoculation with 1% (v/v) culture medium, the samples were cultured at 30 °C and 180 r/min, with OD_{600} measured after 24 hours. To determine the effect of salinity, various concentrations of NaCl were incorporated into the LB medium, resulting in final concentrations of 0%, 0.1%, 1.0%, 5.0%, 10.0%, and 20.0%. Each group was inoculated with 1% (v/v) culture medium and incubated at 30 °C and 180 r/min. After 24 hours, samples were collected and OD_{600} was measured. Each experiment was conducted in triplicate(Xiang et al. 2020).

2.6 Growth-promoting characteristics of different strains

Determination of protease-producing ability: The strain was inoculated to the surface of the protease-producing medium with an inoculation ring, and cultured in an inverted incubator at 30 °C for 2 days. The transparent circle was observed, and the diameter of the transparent circle(D) and the colony diameter(d) were measured respectively. According to the D/d ratio, the protease production capacity of the strain was preliminarily determined(Han et al. 2024).

Determination of amylase ability: The strain was spotted on the amylase-producing selective medium and cultured in an inverted incubator at 30 °C. After 2 d of continuous observation, the plate was taken out and stained with iodine solution to measure the ratio of transparent circle diameter (D) to colony diameter (d)(Soy et al. 2021).

Measurement of cellulase activity: The strain was inoculated on the cellulose Congo red medium and cultured at 30 °C for 2 days. The formation of transparent circles around the colony was observed. The ability of the strain to decompose cellulose was determined by calculating the ratio of the diameter of the transparent circle to the diameter of the colony(Silva et al. 2020).

Assay of siderophore-producing ability: The strain was inoculated on CAS medium and cultured at 30 °C for 9 days. If a yellow transparent circle was formed around the colony, it indicated that the strain had the ability to produce siderophore. The ability of the strain to produce siderophore was determined by calculating the ratio of the diameter of the yellow transparent circle (D) to the diameter of the colony (d)(Gu et al. 2021).

Determination of nitrogen-fixing function: The strains were picked and inoculated on nitrogen-fixing medium, repeated three times, and cultured at 28 °C for 4 days. The growth of bacteria and whether there was a transparent circle at the edge of the colony were observed, and the nitrogen-fixing ability of the strains was judged by the ratio of the diameter of the transparent circle (D) to the diameter of the colony (d)(Arkhipov et al. 2024).

Determination of potassium-solubilizing ability: The strains to be tested were inoculated on the potassium-solubilizing medium, and each strain was repeated three times. The strains with potassium-solubilizing ability were cultured in an inverted incubator at 30 °C for 4 days. A transparent circle appeared around the strains, and the potassium-solubilizing ability was judged by the ratio of the diameter of the transparent circle (D) to the diameter of the colony (d)(Sun et al. 2020).

Quantitative assay of phosphate solubilization: The strains were inoculated into Mengjinna organic phosphorus and inorganic phosphorus medium, and cultured in a constant temperature incubator at 30 °C for 4 days. The diameter of the transparent ring (D) and the diameter of the colony (d) were measured, and the phosphate-solubilizing index (the ratio of the diameter of the transparent ring/the diameter of the colony) was calculated. At the same time, the quantitative analysis experiment was carried out. The strains to be tested were inoculated in LB liquid medium and cultured in a constant temperature shaker at 30 °C and 180 r/min for 1 day as seed solution. The seed solution was inoculated into Mengjinna medium at a volume ratio of 1%, cultured at 30 °C and 180r/min for 3 days, and centrifuged at 8500 r/min for 2 min. The supernatant was taken and the amount of phosphorus was determined by molybdenum antimony colorimetric method(Xu et al. 2026).

IAA-producing ability of strains: Salkowski colorimetric method was used to screen IAA-producing bacteria. The strain was inoculated in a liquid medium containing L-tryptophan (100 mg/L), cultured at 30 °C and 180 r/min for 1 day, and 1 mL bacterial suspension was added to a 24-well plate. At the same time, an equal volume of Salkowski colorimetric solution (50 mL 35% H_2SO_4 + 1 mL 0.5 mol/L $FeCl_3$) was added, and 1mL liquid medium containing L-tryptophan (100 mg/L) was added as a control. The 24-well plate was placed at room temperature away from light for 30 min and observed. The color turned pink was positive, and the darker the color was, the higher the IAA concentration was (Wang et al. 2023).

The ability of the strain to produce biofilm: 2 μL of logarithmic growth phase bacterial solution was added to 2 mL

LBGM medium (tryptone 10 g/L, yeast extract 5 g/L, NaCl 10 g/L, 0.1 mmol/L $MnSO_4$, 1% glycerol, pH 7.0) in 24-well cell culture plates. The cells were cultured at room temperature for 48 h, and the morphology of the capsule was observed and photographed(Wang et al. 2023).

2.7 Whole genome sequencing and analysis

The genomic DNA of the target strain was extracted using a bacterial genomic DNA extraction kit. After passing the quality control test, whole genome high-throughput sequencing was conducted by Shanghai Meiji Technology Co., Ltd. Library construction and sequencing were completed by integrating the PacBio Sequel third-generation sequencing platform with the Illumina NovaSeq second-generation sequencing platform. The genome assembly was performed on the original sequencing data, and the assembled genome sequence was compared with six public databases: SWISS-PROT, COG, PFAM, NR, GO, and KEGG, to facilitate gene prediction and functional annotation. The antiSMASH 5.1.2 software was employed to predict the gene clusters involved in the synthesis of secondary metabolites, and the functional genes associated with the degradation of benzoic acid and other phenolic acids in the strain were predicted and analyzed.

2.8 Pot experiments

Tomato seedlings were transplanted into flowerpots filled with sterile vermiculite, with four plants per pot. The experiment comprised four treatments: the control (CK) group, which was irrigated with clear water; the benzoic acid treatment group, which was watered with benzoic acid (20 mg/kg); the T1 group, which was irrigated with a suspension containing benzoic acid and FJAT-49528 bacteria; and the T2 group, which received a suspension containing benzoic acid and FJAT-53808 bacteria. Each treatment was replicated three times. The temperature of the tissue culture room was maintained at 25 °C, with a 12-hour light/dark cycle.

Determination of growth characteristics in tomato seedlings: Plant height and stem diameter were measured weekly, commencing from the initiation of treatments. Leaf enzyme activity was quantified at the conclusion of the experimental period for each treatment group.

2.9 Statistical analysis

All data were analyzed using SPSS v23.0 software. Initially, tests for homogeneity of variance and normality were conducted on each index data. Subsequently, one-way variance (ANOVA) was employed to compare differences among the various treatment groups. The results are expressed as mean ± standard error (Mean ± SE). Statistically significant differences were defined at the $p < 0.05$ level, with all significance tests being two-tailed.

3. Results and analysis

3.1 Screening for degrading bacteria

Using benzoic acid as the sole carbon source, we screened 19 bacterial strains with ablitiy to degrade benzoic acid. Eventually, we identifed 11 strains that exhibited better growth performance. The degradation effects of 11 strains on benzoic acid were evaluated at different time points. As shown in Figure 1, strains FJAT-49528 and FJAT-53808 demonstrated remarkable degradation capabilities.

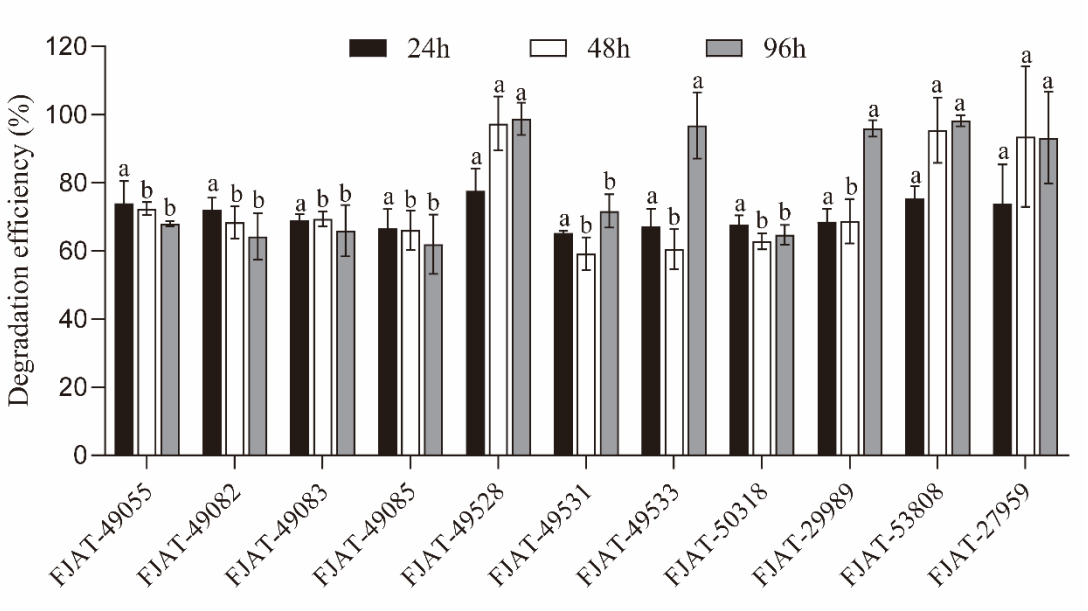


Fig. 1 Degradation abilities of 11 strains to benzoic acid

3.2 Degradation properties of strains FJAT-49528 and FJAT-53808

The benzoic acid degradation rates of both FJAT-49528 and FJAT-53808 showed a gradual increase as the benzoic acid concentration rose from 0.1 g/L to 2.0 g/L (Fig 2a). Their benzoic acid degradation rates reached the maximum at the concentration of 2.0 g/L, which were 93.75% and 95.01%, respectively.

Figure 2b illustrates the degradation effects of FJAT-49528 and FJAT-53808 on four different phenolic acid substrates. FJAT-49528 exhibits a degradation effect on salicylic acid, PHBA, cinnamic acid, and ferulic acid, with PHBA demonstrating the highest degradation rate of 36.88%. In contrast, FJAT-53808 is capable of degrading salicylic acid, PHBA, and cinnamic acid, with the most significant degradation observed in cinnamic acid at a rate of 62.18%. However, FJAT-53808 exhibits no degradation effect on ferulic acid.

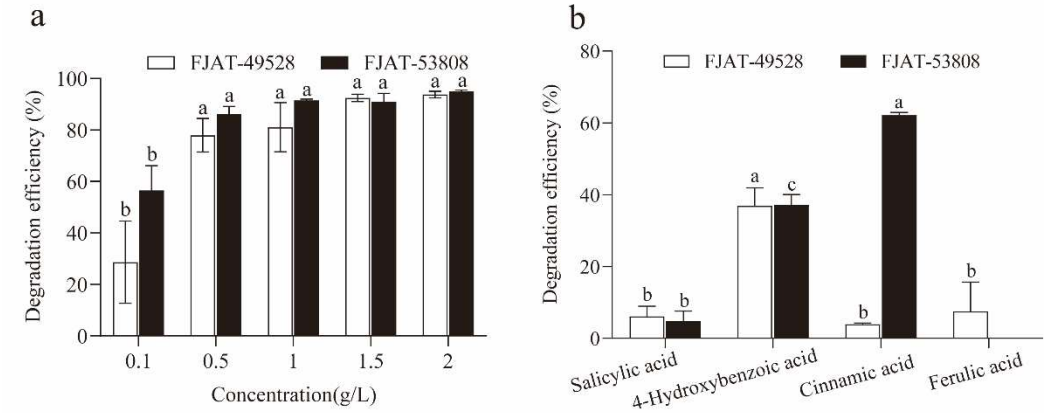


Fig. 2 Degradation ability and degradation spectrum of FJAT-49528 and FJAT-53808.（a.Degradation abilit; b.degradation spectrum）

3.3 Identification of strains FJAT-49528 and FJAT-53808

The colony of strain FJAT-49528 was round or nearly round, presenting a milky-white color, an opaque texture, and a rough and dull surface (Fig. 3a). The cells were in the shape of short rod with a length of 1-2 μm and a width of 0.5-0.6 μm (Fig. 3b). The 16S rRNA gene sequencing and phylogenetic analysis revealed that strain FJAT-49528 (PZ096167) clustered with several published strains of *P. frigoritolerans*, namely MF620091.1, MK696259.1, and OP413033.1, within the same branch (Fig. 3e), indicating a close phylogenetic relationship. The branch node self-expansion value was 55, and the sequence similarity reached up to 99.79%. Based on the phylogenetic clustering characteristics and sequence homology data, it can be concluded that strain FJAT-49528 is classified as *P. frigoritolerans*.

The colony of strain FJAT-53808 was milky white, round, with neat and smooth edges, and exhibited a moist and shiny surface (Fig. 3c). The cells were also in the shape of short rod-shaped with a length of 1.5-2.5 μm and a width of 0.5-0.8 μm (Fig. 3d).The phylogenetic tree constructed based on the 16S rRNA gene sequence (Fig. 3f) indicated that strain FJAT-53808 (PZ363213) and *P. simplex* (OM362934.1) are closely related within the same evolutionary branch. The bootstrap value for this branch was as high as 99, indicating a strong genetic relationship between the two strains. The sequence homology similarity between FJAT-53808 and the model strain reached 99.3%, which can be determined based on phylogenetic clustering rules and sequence homology characteristics. Consequently, strain FJAT-53808 is classified under *P. simplex* in terms of taxonomic status.

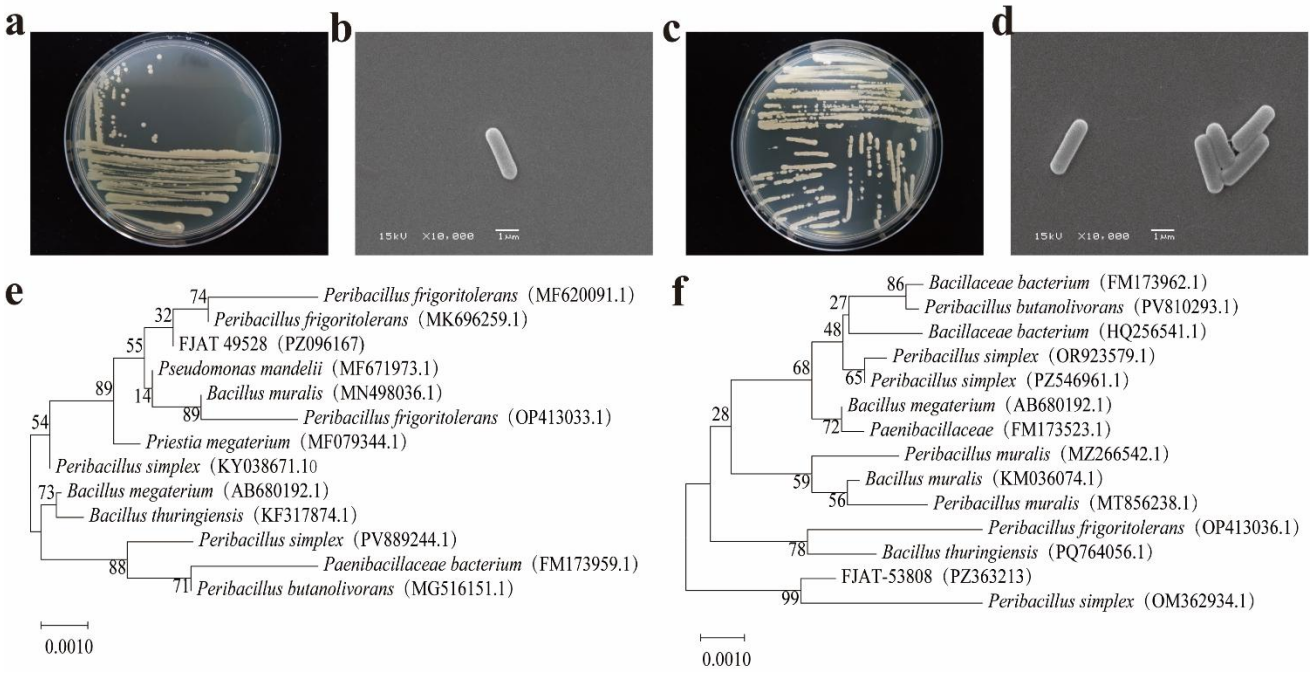


Fig. 3 Colony and cell morphology and the phylogenetic trees of FJAT-49528 and FJAT-53808. a and b were the colony and cell morphology of FJAT-49528; c and d were the colony and cell morphology of FJAT-53808; e and f were the phylogenetic trees of FJAT-49528 and FJAT-53808 based on 16S rRNA nucleotide sequences.

3.4 Genome characteristics and analysis of strains FJAT-49528 and FJAT-53808

The genome assembly indicated that FJAT-49528 contains a circular chromosome (Fig. 4a) with a length of 5,975,191 bp and has a GC content of 40.17%. Similarly, FJAT-53808 was also found to have a circular chromosome (Fig. 4b), measuring 6,089,983 bp with a GC content of 38.02%. The genomes of FJAT-49528 and FJAT-53808 were functionally annotated using COG database. For FJAT-49528, a total of 4,529 genes were annotated, representing 79.43% of the total predicted genes, and were classified into 23 categories (Fig. 4c). Similarly, in FJAT-53808, 4,480 genes were annotated, corresponding 77.36% of the total predicted genes, and also divided into 23 major categories (Fig. 4d).

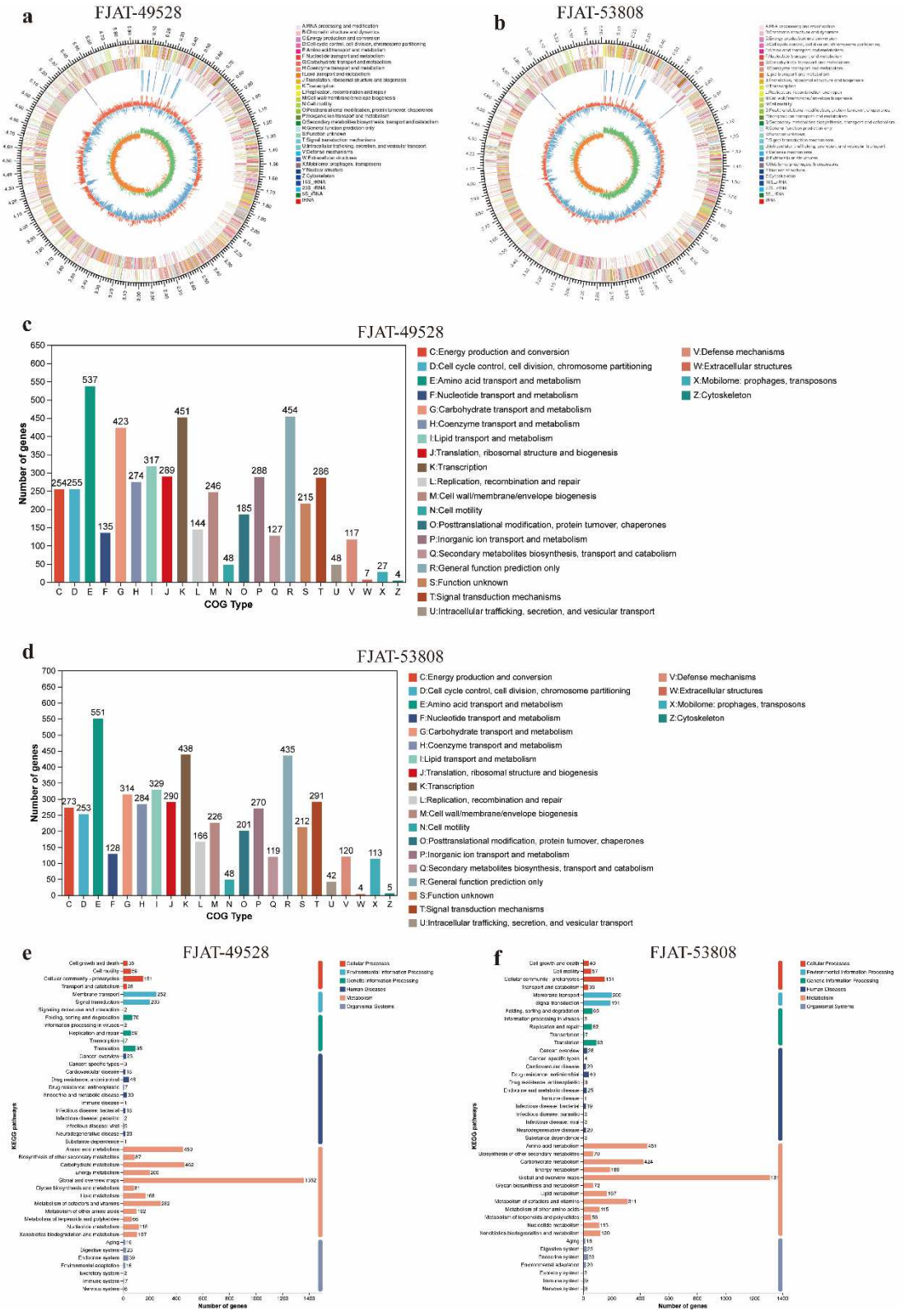


Fig. 4 Genome features and functional annotation analysis of FJAT-49528 and FJAT-53808.

Using the antiSMASH software, secondary metabolite biosynthetic gene clusters were predicted in the whole genomes of strains FJAT-49528 and FJAT-53808, identifying 11 (Fig. 6a) and 8 gene clusters (Fig. 6b), respectively. These clusters included various types such as NRPS, β-lactone, T3PKS, terpene, lasso peptide, LAP, and siderophore. Additionally, strain FJAT-49528 contained one RiPP-like gene cluster. The number of genes encoded by each cluster ranged from 7 to 45. Four types of gene clusters shared between FJAT-49528 and FJAT-53808 matched known functions in the MIBiG database; strain FJAT-49528 also matched an NRPS gene cluster associated with bacillibactin, exhibiting a similarity of 53%. The

highest homologous product identified for both strains was koranimine, with a sequence similarity of 87% (Tables 1 and 2).

Table. 1 Prediction of Secondary Metabolite Biosynthetic Gene Clusters in Strain FJAT-49528

Cluster ID	Type	Start	End	MIBiG accession	Similar Cluster (Similarity/%)	Gene No.
cluster1	NRPS	216793	260777	BGC0000309	bacillibactin(53)	34
cluster2	NRPS	686018	746346	BGC0000377	koranimine(87)	45
cluster3	RiPP-like	2120365	2130976	-	-	7
cluster4	betalactone	2532794	2561937	-	-	34
cluster5	betalactone	2663168	2687338	BGC0001095	fengycin(46)	23
cluster6	T3PKS	3702089	3743178	-	-	40
cluster7	terpene	3882173	3902018	-	-	21
cluster8	lassopeptide	4115986	4139948	BGC0001356	paeninodin(83)	17
cluster9	LAP	4933199	4956735	-	-	16
cluster10	terpene	5558927	5580823	-	-	18
cluster11	siderophore	5914729	5930243	BGC0001196	desotamide(9)	13

Table. 2 Prediction of Secondary Metabolite Biosynthetic Gene Clusters in Strain FJAT-53808

Cluster ID	Type	Start	End	MIBiG accession	Similar Cluster (Similarity/%)	Gene No.
cluster1	NRPS	644872	705210	BGC0000377	koranimine（87）	37
cluster2	betalactone	2559198	2583408	BGC0001095	fengycin（46）	22
cluster3	T3PKS	3446031	3487120	-	-	39
cluster4	terpene	3616512	3636215	-	-	19
cluster5	lassopeptide	3838942	3862990	BGC0001356	paeninodin（83）	22
cluster6	LAP	4587709	4611244	-	-	17
cluster7	terpene	5089355	5111254	-	-	16
cluster8	siderophore	5455612	5471126	BGC0001196	desotamide（9）	14



Fig. 5 Gene cluster diagram of secondary metabolite biosynthesis.

3.4.2 Key genes information related to phenolic acid degradation

Genomic functional annotation revealed that both FJAT-49528 and FJAT-53808 harbor key genes involved in the benzoate degradation pathway. Both strains carry the benzoate transport protein-encoding gene *benK*, the benzoyl-CoA ligase-encoding gene *badA*, and the demethylase-encoding gene *desA*, which enable extracellular transport, *CoA* activation, and the demethylation degradation of benzoate. In the 4-hydroxybenzoate (PHBA) degradation pathway, both strains possess the core gene *pcaD*, which encodes β-ketoadipate enol-lactone hydrolase, a key enzyme responsible for the ring-cleavage of phenolic acids. Additionally, FJAT-49528 carries genes *pcaC*, *pcaF*, *pcaR*, and *pcaI*, while FJAT-53808 carries genes *pcaC*, *pcaF*, and *pcaR*, collectively constituting a complete PHBA degradation module. Furthermore, FJAT-49528 was annotated with genes involved in the degradation pathways of catechol, phenylacetate, hydroxyphenylacetate, phenylpropionate, phenol, salicylate, and gallate, whereas FJAT-53808 was annotated with genes involved in the degradation pathways of catechol, gentisate, phenylacetate, hydroxyphenylacetate, phenylpropionate, phenol, vanillate, and salicylate. These results indicate that both strains possess abundant gene resources for the degradation of aromatic compounds, exhibiting potential application value in the degradation of phenolic acid autotoxic substances and the remediation of continuous cropping obstacles.

Table. 3 Key genes information related to phenolic acid degradation

Factors	Gene ID	Gene Name	function
FJAT-49528			
Benzoate Degradation Pathway	gene0262	*benK*	Benzoate transport protein
	gene2175	*badA*	Benzoate-CoA ligase

	gene2462	*badH*	Benzaldehyde dehydrogenase / 2-hydroxycyclohexanecarboxyl-CoA dehydrogenase
	gene4988	*benM*	Benzoate and cis,cis-muconate-responsive transcriptional activator
Protocatechuate Degradation Pathway	gene0885	*pcaC*	4-carboxymuconolactone decarboxylase
	gene1133	*pcaF*	3-oxoadipyl-CoA thiolase
	gene2383	*pcaD*	3-oxoadipate enol-lactonase
	gene2409	*pcaR*	pca regulon regulatory protein
	gene2410	*pcaI*	3-oxoadipate CoA-transferase, alpha subunit
Catechol Degradation Pathway	gene2262	*catB*	Muconate cycloisomerase
	gene2265	*catA*	Catechol 1,2-dioxygenase
	gene4369	*catE*	Catechol 2,3-dioxygenase
	gene1333	*nagX*	3-hydroxybenzoate 6-monooxygenase
	gene3421	*nagK*	Fumarylpyruvate hydrolase
4-Hydroxybenzoate Degradation	gene2964	*pobR*	Transcriptional activator of pobA
Gallate Degradation	gene2229	*lpdC*	Gallate decarboxylase subunit C
Salicylate Degradation/Response	gene3572	*bsdA*	Salicylic acid-responsive activator of bsdBCD
Hydroxyphenylacetate Degradation Pathway	gene1084	*hpaB*	4-hydroxyphenylacetate 3-monooxygenase
	gene3568	*hpaG*	5-oxopent-3-ene-1,2,5-tricarboxylate decarboxylase / 2-hydroxyhepta-2,4-diene-1,7-dioate isomerase
	gene3570	*hpaF*	5-carboxymethyl-2-hydroxymuconate isomerase
	gene3577	*hpaE*	5-carboxymethyl-2-hydroxymuconic-semialdehyde dehydrogenase
	gene4602	*hpaI*	4-hydroxy-2-oxoheptanedioate aldolase
Phenylpropionate/Hydroxyphenylpropionate Degradation Pathway	gene0892	*mhpC*	2-hydroxy-6-oxonona-2,4-dienedioate hydrolase
	gene2382	*hcaB*	2,3-dihydroxy-2,3-dihydrophenylpropionate dehydrogenase
	gene2452	*mhpD*	2-keto-4-pentenoate hydratase
	gene2454	*mhpE*	4-hydroxy-2-oxovalerate aldolase
Phenol Degradation Pathway	gene2451	*dmpC*	2-hydroxymuconate-6-semialdehyde dehydrogenase
	gene2455	*dmpH*	2-oxo-3-hexenedioate decarboxylase
	gene3576	*dmpB*	Catechol 2,3-dioxygenase
	gene5661	*praC*	4-oxocrotonate tautomerase
Phenylacetate Degradation Pathway	gene1119	*paaI*	Acyl-CoA thioesterase
	gene1122	*paaK*	Phenylacetate-CoA ligase
	gene1124	*paaA*	Ring-1,2-phenylacetyl-CoA epoxidase subunit PaaA

	gene1125	*paaB*	Ring-1,2-phenylacetyl-CoA epoxidase subunit PaaB
	gene1126	*paaC*	Ring-1,2-phenylacetyl-CoA epoxidase subunit PaaC
	gene1127	*paaD*	Ring-1,2-phenylacetyl-CoA epoxidase subunit PaaD
	gene1129	*paaF*	Enoyl-CoA hydratase
	gene1130	*paaG*	2-(1,2-epoxy-1,2-dihydrophenyl)acetyl-CoA isomerase
	gene1132	*paaH*	3-hydroxybutyryl-CoA dehydrogenase
	gene1135	*paaX*	Phenylacetic acid degradation operon negative regulatory protein
Phthalate Degradation	gene2212	*pht3*	Phthalate 4,5-dioxygenase
FJAT-53808			
Benzoate Degradation Pathway	gene1516	*benK*	Benzoate transport protein
	gene1999	*badA*	Benzoate-CoA ligase
	gene2377	*badH*	Benzaldehyde dehydrogenase / 2-hydroxycyclohexanecarboxyl-CoA dehydrogenase
Protocatechuate Degradation Pathway	pA_gene0043	*pcaD*	3-oxoadipate enol-lactonase
	gene0776	*pcaC*	4-carboxymuconolactone decarboxylase
	gene1044	*pcaF*	3-oxoadipyl-CoA thiolase
	gene2444	*pcaR*	pca regulon regulatory protein
Catechol Degradation Pathway	gene0454	*catE*	Catechol 2,3-dioxygenase
	pA_gene0062	*nagX*	3-hydroxybenzoate 6-monooxygenase
	pA_gene0063	*E1.13.11.4*	Gentisate 1,2-dioxygenase
	gene2903	*nagK*	Fumarylpyruvate hydrolase
Vanillate Degradation	gene2090	*vanR*	Vanillate catabolism transcriptional regulator
Salicylate Degradation/Response	pA_gene0009	*bsdA*	Salicylic acid-responsive activator of bsdBCD
Hydroxyphenylacetate Degradation Pathway	gene0783	*hpaG*	5-oxopent-3-ene-1,2,5-tricarboxylate decarboxylase / 2-hydroxyhepta-2,4-diene-1,7-dioate isomerase
Phenylpropionate/Hydroxyphenylpropionate Degradation	pA_gene0083	*mhpE*	4-hydroxy-2-oxovalerate aldolase
	pA_gene0085	*mhpD*	2-keto-4-pentenoate hydratase
	pA_gene0090	*mhpC*	2-hydroxy-6-oxonona-2,4-dienedioate hydrolase

	gene2453	*hcaB*	2,3-dihydroxy-2,3-dihydrophenylpropionate dehydrogenase
Phenol Degradation Pathway	gene2065	*dmpD*	2-hydroxymuconate-semialdehyde hydrolase
	gene5190	*praC*	4-oxalocrotonate tautomerase
Phenylacetate Degradation Pathway	gene1029	*paaI*	Acyl-CoA thioesterase
	gene1032	*paaK*	Phenylacetate-CoA ligase
	gene1035	*paaA*	Ring-1,2-phenylacetyl-CoA epoxidase subunit PaaA
	gene1036	*paaB*	Ring-1,2-phenylacetyl-CoA epoxidase subunit PaaB
	gene1037	*paaC*	Ring-1,2-phenylacetyl-CoA epoxidase subunit PaaC
	gene1038	*paaD*	Ring-1,2-phenylacetyl-CoA epoxidase subunit PaaD
	gene1040	*paaF*	Enoyl-CoA hydratase
	gene1041	*paaG*	2-(1,2-epoxy-1,2-dihydrophenyl)acetyl-CoA isomerase
	gene1043	*paaH*	3-hydroxybutyryl-CoA dehydrogenase
	gene1046	*paaX*	Phenylacetic acid degradation operon negative regulatory protein

3.5 Growth characteristics of strains FJAT-49528 and FJAT-53808

The growth curves of FJAT-49528 and FJAT-53808 was nearly identical (Fig. 7a). Both strains exhibited a lag phase from 0 to 4 h, entered the logarithmic growth phase after 4 h, and reached a plateau at approximately 24 h. FJAT-49528 and FJAT-53808 grew normally in neutral and alkaline environments (pH7-9), with the optimal growth observed at pH 7. Under the same pH conditions, the biomass of FJAT-49528 in the pH9 medium was higher than that of FJAT-53808 (Fig. 7b). Both strains grew efficiently with a NaCl concentration range of 0.0%-2.0% (Fig. 7c). Further investigation showed that FJAT-49528 and FJAT-53808 could grow between 20 °C.and 50 °C. The optimum growth temperature for FJAT-49528 was 30 °C, whereas FJAT-53808 retained measurable growth capacity at 50 °C (Fig. 7d).

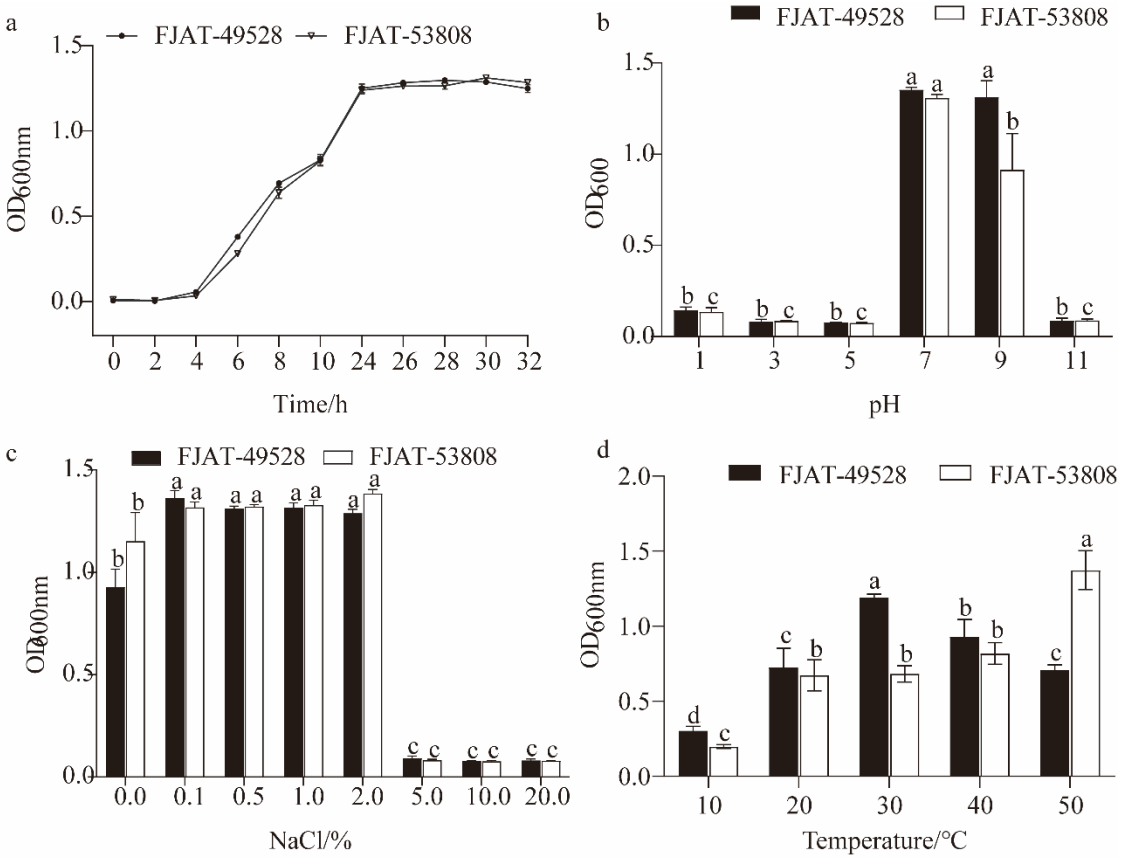


Fig. 6 Growth characteristics and environmental stress tolerance under different conditions. (a.Growth curve; b.pH tolerance; c.Salt stress tolerance; d.Temperature tolerance)

3.6 Growth-promoting characteristics of strains FJAT-49528 and FJAT-53808

Both FJAT-49528 and FJAT-53808 exhibited the abilities to produce indole acetic acid (IAA), siderophore and cellulose, as well as to solubilize organic phosphorus. Additonally, FJAT-53808 also demonstrated nitrogen fixation capability (Table 4 and Fig. 8). The IAA production for FJAT-49528 and FJAT-53808 were 41.81 mg/L and 39.90 mg/L, respectively. The organic phosphorus solubilization capacities of the two strains were 76.90 mg/L and 73.73 mg/L, repectively.

Table. 4 Plant growth-promoting characteristics

Strain	IAA production capacity (mg/L)	The ability to solubilize organic phosphorus (mg/L)	Relative siderophore producing ability
FJAT-49528	41.81±5.17	76.90±2.66	0.47±0.02
FJAT-53808	39.90±7.83	73.73±5.68	0.46±0.03

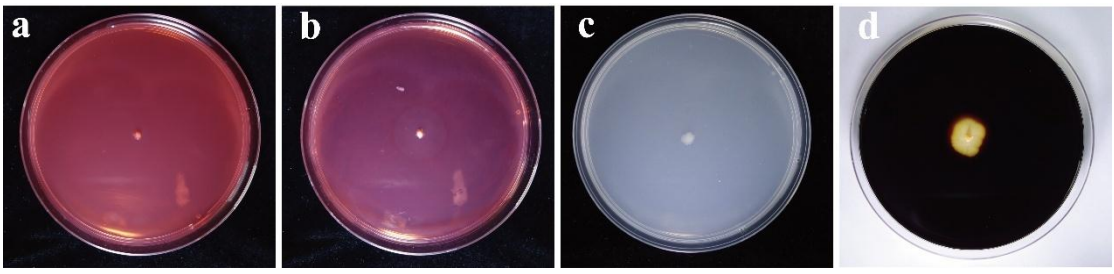


Fig. 7 The growth-promoting characteristics of FJAT-49528 (a.FJAT-49528 cellulase; b, c, d. FJAT-53808 cellulase, nitrogen fixation, siderophore production)

3.7 Effects of FJAT-49528 and FJAT-53808 on tomato growth

3.7.1 Growth-promoting

In the BA group, tomato root growth was inhibitied, with the root system exhibiting yellowing and senescence. In contrast, the application of benzoic acid-degrading bacteria in T1 and T2 groups significantly restored root growth and effectively alleviate the symptoms of root yellowing and senescence. Additionaly, plants in the T1 and T2 groups displayed more luxuriant stems and leaves, significantly improved root length (Fig. 9).

Under conditions of benzoic acid autotoxicity stress, growth indices of tomato plants indicated that the plant height, root length, above ground and root fresh weight, dry weight and stem diameter of the T1 and T2 groups, as well as the CK group, were significantly greater than those in BA group (Fig. 10). Among these treatments, the T2 group exhibited significantly higher plant height and root dry weight compared to all other groups, reaching 33.20 cm and 0.14 g, respectively. Additonaly, root length in both the T1 and T2 treatments was significantly incrased relative to the BA group, measuring 10.73 cm and 11.73 cm, respectively.

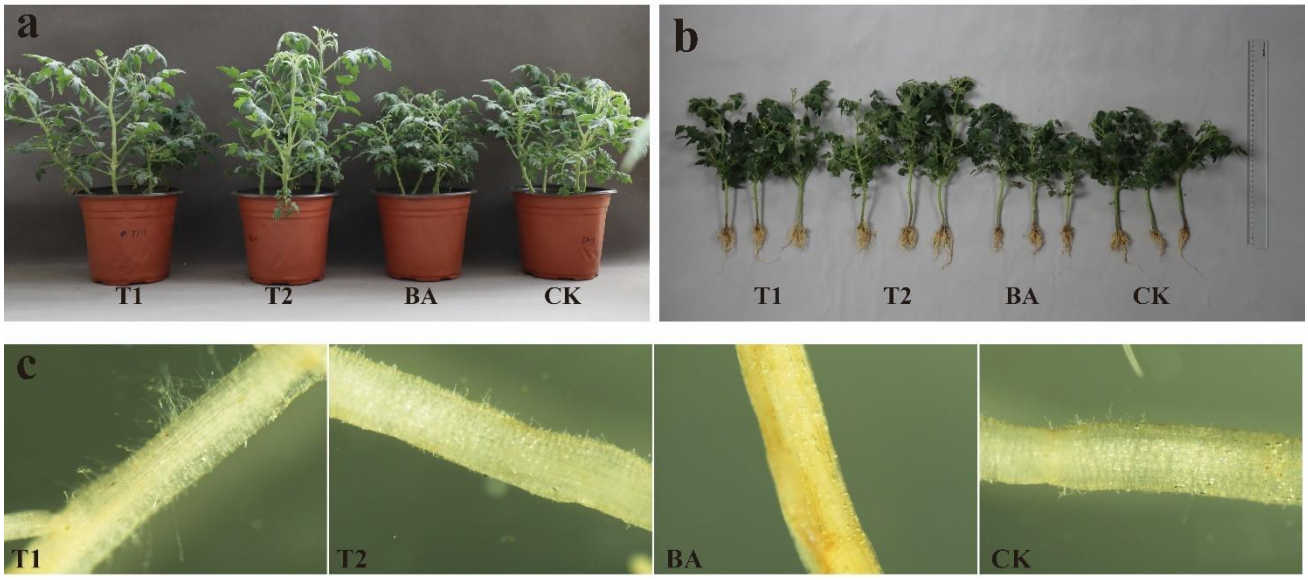


Fig. 8. Phenotypic characteristics of tomato plants and roots after inoculation with two degrading bacteria under benzoic acid stress. (a.plant phenotypic characteristics; b.overall morphology of tomatoes; c.microscopic structure of roots)

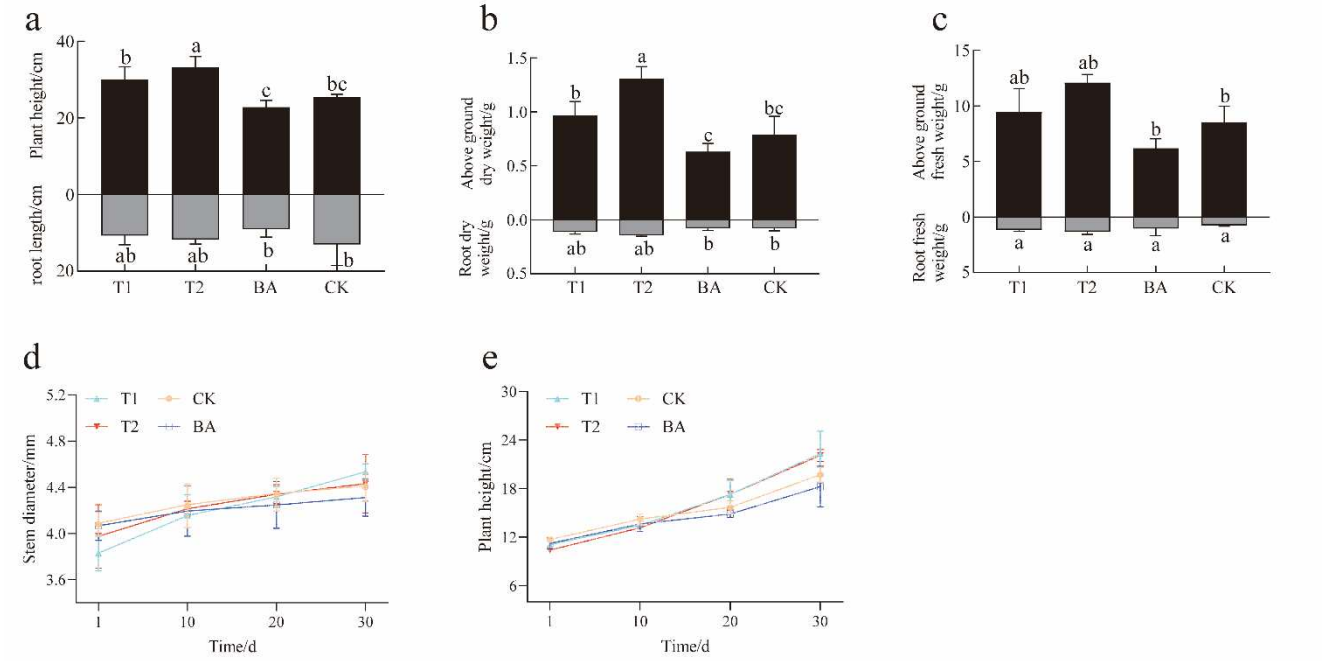


Fig. 9 Growth indicators and dynamic changes of tomato plants under different treatments with benzoic acid stress.(a.plant height and root length; b.dry weight of aboveground and underground parts; c.fresh weight of aboveground and underground parts; d.dynamic changes of stem thickness; e.dynamic changes of plant height)

3.7.2 Enzyme activities

As shown in Figure 11, on day 30, the MDA content in the T1 and T2 groups was measured at 29.29 nmol/g and 30.04 nmol/g, respectively, which represented a significant reduction compared to the CK group (34.13 nmol/g) by 16.5% and 13.6%, effectively inhibiting membrane lipid peroxidation. Following treatment with benzoic acid on day 10, the POD activity decreased to 20.33 U/g in comparison to the CK group, marking a decline of 74.5%. However, the T1 and T2 groups were able to restore the POD activity to 90.33 U/g and 88.67 U/g, respectively. During the same period, the PPO activity in the T1 group reached 401.33 U/g, reflecting an increase of 36.2% compared to the BA group (294.67 U/g). In the later stages of the experiment, the PPO activity in the T1 group remained elevated, while the POD and PPO activities in the T2 group exhibited a stable trend throughout the duration of the study.

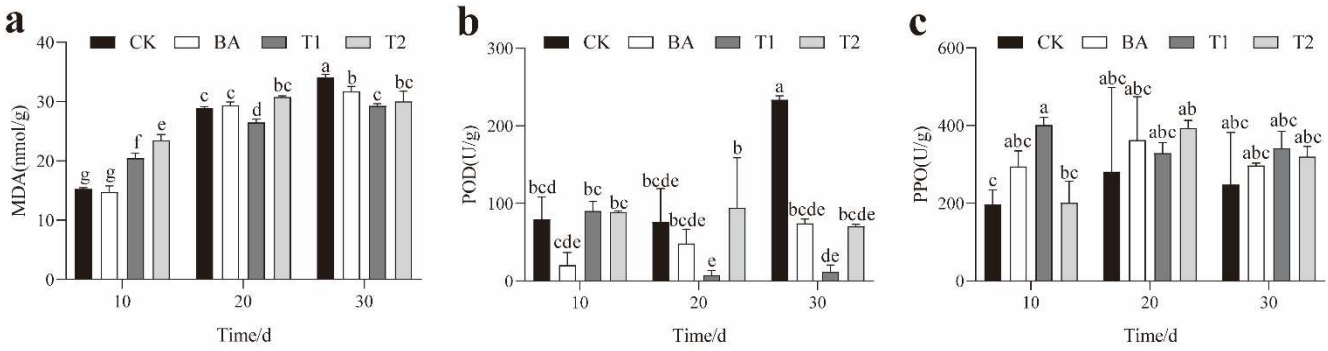


Fig. 10 Dynamic changes of MDA content, POD and PPO activities in tomato leaves under different treatments with benzoic acid stress.

4. Discussion

Continuous cropping obstacles significantly limit crop yield and quality in facility agricultural production, with the accumulation of phenolic acid allelochemicals identified as a key contributing factor(Wang et al. 2026). Benzoic acid, a typical phenolic acid autotoxin, is commonly found in soils subjected to continuous cropping. Its persistent accumulation can inhibit root growth and disrupt the structure of soil microbial communities, thereby exacerbating the prevalence of soil-borne diseases(Zhang et al. 2026). Microbial degradation presents an effective strategy for mitigating the residue of autotoxins. *Bacillus* species have received considerable attention in the development of functional microbial agents due to their advantageous growth characteristics, including strong stress resistance, simple nutritional requirements, and the ability to form endophytic spores(Huang et al. 2018; Wu et al. 2021). Previous studies have demonstrated that various *Bacillus* strains possess the capability to degrade benzoic acid. for example, *Bacillus thermophilus* has been shown to degrade cinnamic acid, ferulic acid, and other phenolic acid allelochemicals(Peng et al. 2003). Additionally, two *Bacillus* strains have been reported to exhibit allelochemical degradation, promote plant growth, and alleviate stress(Iqbal et al. 2025). Furthermore, *B. subtilis* utilizes benzoic acid as a key intermediate during the degradation of naphthenic acid, facilitating ring-opening decomposition(Chauhan et al. 2025). However, research on the application of such degrading bacteria for the prevention and control of tomato continuous cropping obstacles remains relatively limited.

In this study, we screened and obtained benzoic acid-degrading strains *P. frigoritolerans* FJAT-49528 and *P. simplex* FJAT-53808. Substrate concentration gradient experiments demonstrated that as the concentration of benzoic acid increased, the degradation efficiency of both strains gradually improved. They also exhibited varying degrees of degradation ability towards different phenolic acid autotoxins, including salicylic acid, cinnamic acid, and PHBA, with PHBA showing the highest degradation efficacy. Numerous studies have confirmed that *Bacillus* species generally possess the capability to degrade phenolic acid allelochemicals. For instance, *Bacillus subtilis* and *Pseudomonas* are known to effectively degrade autotoxic substances such as soil benzoic acid and PHBA(Kitko et al. 2009; Zhang et al. 2025). However, there is currently no systematic report on the phenolic acid degradation capabilities of *P. frigoritolerans* and *P. simplex*. The findings of this study contribute to the germplasm resources of efficient degrading bacteria that can be utilized to address challenges associated with continuous tomato cropping.

FJAT-49528 and FJAT-53808 are both monocyclic chromosome genomes that demonstrate an efficient degradation effect on benzoic acid. Previous studies have elucidated the degradation pathways and key functional genes of phenolic acids in various *Bacillus* strains. However, the genome-wide characteristics and functional gene system analysis of the two

Bacillus strains used in this study have not been reported. Functional annotations using COG and KEGG revealed that the genomes of the two strains are enriched with numerous coding genes related to carbohydrate transport metabolism, amino acid metabolism, and inorganic ion transport. This characteristic has been documented in many types of rhizosphere growth-promoting *Bacillus*, providing a genetic basis for the strains to utilize various carbon sources in the rhizosphere, activate soil nutrients, and adapt to the stress conditions of the rhizosphere(Jadeja et al. 2019; Escalante-Beltrán et al. 2026). AntiSMASH predicted numerous secondary metabolite synthesis gene clusters, many of which exhibited high homology to known antimicrobial lipopeptide, lassopeptide, and siderophore synthesis genes, thereby elucidating the nutritional competitiveness of the two strains *in vitro*. Additionally, many studies have reported the presence of abundant secondary metabolite synthesis gene resources in the genomes of *Bacillus*(Ghimire et al. 2022; Liu et al. 2025). In this study, key genes involved in phenolic acid degradation, such as *pcaD*, *benK*, and *desA*, were annotated in the genome of FJAT-49528, while the key genes *pcaD* and *desA* were annotated in FJAT-53808, endowing the strains with the genetic potential to efficiently degrade autotoxic substances like benzoic acid and ρ-hydroxybenzoic acid.

The environmental adaptability of the functional strain is a fundamental factor in determining its capacity to colonize fields and its efficacy in application. This study examined the growth characteristics of FJAT-49528 and FJAT-53808. The growth dynamics of both strains were similar, as they rapidly entered the logarithmic growth phase around 4 h, enabling them to quickly colonize the rhizosphere and establish a dominant microbial community. The optimal growth pH for both strains was found to be 7, with an ideal growth temperature of 30 °C. Both strains exhibited tolerance to NaCl salt stress up to 2%, enabling their adaptation to neutral to mildly alkaline and slightly saline soil environments commonly found in many botanical gardens. Previous research indicates that the ideal growth conditions for most agricultural *Bacillus* species are characterized by neutral temperatures, neutral pH, and low salt stress(Carlin et al. 2013; Li et al. 2024b), which aligns with the findings of this study. FJAT-49528 exhibited a greater growth advantage under mildly alkaline conditions, making it more suitable for conventional field cultivation, while FJAT-53808 displayed some resistance to high temperatures, offering advantages for soil remediation applications during warmer seasons.

The strain FJAT-49528 can secrete a significant amount of IAA, measured at 41.81 mg/L, which promotes the development of plant roots and enhances the ability of plants to absorb soil water and nutrients. Numerous studies have confirmed that *Bacillus* strains exhibit growth-promoting characteristics through efficient IAA secretion(Wang et al. 2021). Both strains are capable of synthesizing siderophores, which provide bioavailable iron to support plant growth. Strains FJAT-49528 and FJAT-53808 demonstrate a strong ability to dissolve organic phosphorus, converting insoluble organic phosphorus in the soil into a form that can be absorbed and utilized by plants. This phosphorus-dissolving capability has been documented in various *Bacillus* strains, including *B. amyloliquefaciens*(Ben Abdallah et al. 2018), *B. subtilis*(Ahmad et al. 2017), and *Bacillus pumilus*(Ansari et al. 2019). Furthermore, both strains can produce cellulase, and FJAT-53808 possesses additional biological nitrogen fixation abilities, which can further activate soil nitrogen, improve the nutrient status of rhizosphere soil, and help mitigate the challenges associated with continuous cropping that threaten the healthy growth of crops.

Allelochemicals that accumulate in rhizosphere soil can exert toxic effects on plant growth, inhibiting seed germination and seedling development of the same crop(Tu et al. 2023). This study conducted pot experiments to investigate the toxic effects of benzoic acid on tomato plants, as well as the effects of inoculating degrading strains FJAT-49528 and FJAT-53808. The results indicated that benzoic acid stress significantly inhibited tomato growth, leading to yellowing and senescence of roots, alongside a marked decrease in plant height and biomass. Inoculation with FJAT-49528 and FJAT-53808 markedly restored the growth of tomato shoots and roots, effectively alleviating the toxic damage caused by phenolic acids. Numerous studies have confirmed that rhizobacteria possessing both phenolic acid degradation and growth-promoting functions can ameliorate crop growth disorders under autotoxic stress by improving the rhizosphere microenvironment and activating soil nutrients(Liu et al. 2017; Duan et al. 2022; Yang et al. 2026). The physiological indices of MDA, POD, and PPO revealed that the two strains enhanced the tolerance of tomatoes to phenolic acid stress by activating the endogenous antioxidant defense system, reducing damage from cell membrane lipid peroxidation, and improving the activity of defense enzymes. This finding aligns with previous research on the physiological responses of crops induced by biocontrol *Bacillus*(Aldayel et al. 2024).

5. Conclusion

In summary, the two benzoic acid-degrading strains FJAT-49528 and FJAT-53808 screened in this study were identified as *P. frigoritolerans* and *P. simplex* by 16S rRNA identification and phylogenetic analysis. In addition to their high ability to degrade benzoic acid, they also showed the potential to promote plant growth. Furthermore, via genome mining and comprehensive comparative analysis, numerous genes associated with autotoxicity degradation and plant probiotics were identified, providing a reliable fundation for further exploration. Our research offers support for further investigation and application of phenolic acid-degrading microorganisms to mitigate agricultural continuous cropping obstacles.

CRediT authorship contribution statement:

Jianmei Che: Writing – review & editing, Supervision, Project administration, Funding acquisition, Conceptualization. Dongliang Qiu: Writing – review & editing. Miaomiao Liu: Writing – review & editing, Writing – original draft, Visualization, Validation, Investigation. Junhao Huang: Validation, Data curation. Xuefang Zheng: Writing – review & editing. Jieping Wang: Writing – review & editing, Software. Yanping Chen: Methodology.

Declaration of Competing Interest

The authors declare no competing interests.

Funding

This work was financed by Special Project for the Construction of Provincial Germplasm Resources Conservation Units in Fujian Province (ZYBHDWZX202601), Fujian Province's Spark Program Project (2025S0003) and Key Agricultural Guiding Project of Fujian Province (2024N0068).

Data availability Statement:

All data is contained within the article.

Reference

Ahmad Z, Wu J, Chen L, Dong W (2017) Isolated *Bacillus subtilis* strain 330-2 and its antagonistic genes identified by the removing PCR. Sci Rep 7:1777. https://doi.org/10.1038/s41598-017-01940-9

Aldayel MF, Alrajeh HS, Sallam NMA, Imran M (2024) *Bacillus Amyloliquefaciens* IKMM and Zinc Nanoparticles as Biocontrol Candidate Induce the Systemic Resistance by Producing Antioxidants in Tomato Plants Challenged with Early Blight Pathogen. J Crop Health 76:87–103. https://doi.org/10.1007/s10343-023-00942-0

An X, Wang Y, Yu C, Hu X (2024) Biochar-bacteria coupling system enhanced the bioremediation of phenol wastewater-based on life cycle assessment and environmental safety analysis. J Hazard Mater 480:136414. https://doi.org/10.1016/j.jhazmat.2024.136414

Ansari FA, Ahmad I, Pichtel J (2019) Growth stimulation and alleviation of salinity stress to wheat by the biofilm forming *Bacillus pumilus* strain FAB10. Appl Soil Ecol 143:45–54. https://doi.org/10.1016/j.apsoil.2019.05.023

Arkhipov A, Shao Z, Muirhead SR, et al (2024) Microbe-Friendly Plants Enable Beneficial Interactions with Soil Rhizosphere Bacteria by Lowering Their Defense Responses. Plants 13:3065. https://doi.org/10.3390/plants13213065

Aromokeye DA, Oni OE, Tebben J, et al (2021) Crystalline iron oxides stimulate methanogenic benzoate degradation in marine sediment-derived enrichment cultures. ISME J 15:965–980. https://doi.org/10.1038/s41396-020-00824-7

Ben Abdallah D, Frikha Gargouri O, Tounsi S (2018) Rizhospheric competence, plant growth promotion and biocontrol efficacy of *Bacillus amyloliquefaciens* subsp. *plantarum* strain 32a. Biol Control 124:61–67.

https://doi.org/10.1016/j.biocontrol.2018.01.013
Carlin F, Albagnac C, Rida A, et al (2013) Variation of cardinal growth parameters and growth limits according to phylogenetic affiliation in the *Bacillus cereus* Group. Consequences for risk assessment. Food Microbiol 33:69–76. https://doi.org/10.1016/j.fm.2012.08.014
Chauhan P, Kanaujia PK, Suman SK (2025) Bioremediation of naphthenic acid by *Bacillus subtilis*: Degradation kinetics and pathway elucidation. Environ Pollut 376:126383. https://doi.org/10.1016/j.envpol.2025.126383
Duan Y, Zhou Y, Li Z, et al (2022) Effects of *Bacillus amyloliquefaciens* QSB-6 on the Growth of Replanted Apple Trees and the Soil Microbial Environment. Horticulturae 8:83. https://doi.org/10.3390/horticulturae8010083
Emelyanova EV, Ramanaiah SV, Prisyazhnaya NV, et al (2023) The Contribution of Actinobacteria to the Degradation of Chlorinated Compounds: Variations in the Activity of Key Degradation Enzymes. Microorganisms 11:141. https://doi.org/10.3390/microorganisms11010141
Escalante-Beltrán A, Morales-Sandoval PH, Montoya-Martínez AC, et al (2026) Draft genome sequence of *Bacillus* sp. Strain 11B20, a promising plant-growth promoting bacterium associated with maize (zea mays L.) in the yaqui valley, mexico. Microorganisms 14:485. https://doi.org/10.3390/microorganisms14020485
Esikova TZ, Anokhina TO, Abashina TN, et al (2021) Characterization of Soil Bacteria with Potential to Degrade Benzoate and Antagonistic to Fungal and Bacterial Phytopathogens. Microorganisms 9:755. https://doi.org/10.3390/microorganisms9040755
Ghimire N, Kim B, Lee C, Oh T (2022) Comparative genome analysis among *Variovorax* species and genome guided aromatic compound degradation analysis emphasizing 4-hydroxybenzoate degradation in *Variovorax* sp. PAMC26660. BMC Genomics 23:375. https://doi.org/10.1186/s12864-022-08589-3
Gu S, Wan W, Shao Z, Wei Z (2021) High-throughput Method for Detecting Siderophore Production by Rhizosphere Bacteria. BIO-PROTOC 11:. https://doi.org/10.21769/BioProtoc.4001
Han Y, Li Y, Qiu W, et al (2024) Integrated whole genome sequencing and transcriptomic analysis reveal the biodegradation mechanism of vanillic acid in *Herbaspirillum aquaticum* KLS-1. J Environ Chem Eng 12:113221. https://doi.org/10.1016/j.jece.2024.113221
Hu C, Lv Y, Xian W, et al (2024) Multi-omics insights into the function and evolution of sodium benzoate biodegradation pathway in Benzoatithermus flavus gen. nov., sp. nov. from hot spring. J Hazard Mater 476:135017. https://doi.org/10.1016/j.jhazmat.2024.135017
Huang Y, Xiao L, Li F, et al (2018) Microbial Degradation of Pesticide Residues and an Emphasis on the Degradation of Cypermethrin and 3-phenoxy Benzoic Acid: A Review. Molecules 23:2313. https://doi.org/10.3390/molecules23092313
Iqbal S, Begum F, Manishimwe C, et al (2025) Allelochemicals degradation and multifarious plant growth promoting potential of two *Bacillus* spp.: Insights into genomic potential and abiotic stress alleviation. Chemosphere 373:144191. https://doi.org/10.1016/j.chemosphere.2025.144191
Jadeja NB, Moharir P, Kapley A (2019) Genome Sequencing and Analysis of Strains *Bacillus* sp. AKBS9 and *Acinetobacter* sp. AKBS16 for Biosurfactant Production and Bioremediation. Appl Biochem Biotechnol 187:518–530. https://doi.org/10.1007/s12010-018-2828-x
Jiang W, Chen R, Zhao L, et al (2022) Chemical fumigants control apple replant disease: Microbial community structure-mediated inhibition of *Fusarium* and degradation of phenolic acids. J Hazard Mater 440:129786. https://doi.org/10.1016/j.jhazmat.2022.129786
Kitko RD, Cleeton RL, Armentrout EI, et al (2009) Cytoplasmic Acidification and the Benzoate Transcriptome in *Bacillus subtilis*. PLOS One 4:e8255. https://doi.org/10.1371/journal.pone.0008255
Li H, Lou J, Chen X, et al (2024a) Effects of sweet pepper straw biochar on soil microbial communities and growth of continuously cropped cucumber. Ann Microbiol 74:12. https://doi.org/10.1186/s13213-024-01755-w

Li Q, Huang Z, Zhong Z, et al (2024b) Integrated Genomics and Transcriptomics Provide Insights into Salt Stress Response in *Bacillus subtilis* ACP81 from Moso Bamboo Shoot (Phyllostachys praecox) Processing Waste. Microorganisms 12:285. https://doi.org/10.3390/microorganisms12020285

Li R, Zhang N, Deng X, et al (2024c) Tomato bacterial wilt disease outbreaks are accompanied by an increase in soil antibiotic resistance. Environ Int 190:108896. https://doi.org/10.1016/j.envint.2024.108896

Li Y, Ren Y, Jiang N (2017) Analysis of Draft Genome Sequence of *Pseudomonas* sp. QTF5 Reveals Its Benzoic Acid Degradation Ability and Heavy Metal Tolerance. Biomed Res Int 2017:1–7. https://doi.org/10.1155/2017/4565960

Liu D, Ge X, Pan D, et al (2024) *Bacillus subtilis* B55 degraded the ferulic acid and *p*-coumaric acid and changed the soil bacterial community in soils. J Appl Microbiol 135:lxae243. https://doi.org/10.1093/jambio/lxae243

Liu J, Wang X, Zhang T, Li X (2017) Assessment of active bacteria metabolizing phenolic acids in the peanut (*Arachis hypogaea* L.) rhizosphere. Microbiol Res 205:118–124. https://doi.org/10.1016/j.micres.2017.09.005

Liu X, Sun L, Wang S, et al (2025) Genomic analysis and phytoprobiotic characteristics of *Acinetobacter pittii* P09: A p-hydroxybenzoic acid-degrading plant-growth promoting rhizobacteria. Environ Technol Innovation 38:104113. https://doi.org/10.1016/j.eti.2025.104113

Mpofu E, Chakraborty J, Suzuki-Minakuchi C, et al (2019) Biotransformation of Monocyclic Phenolic Compounds by *Bacillus licheniformis* TAB7. Microorganisms 8:26. https://doi.org/10.3390/microorganisms8010026

Peng X, Misawa N, Harayama S (2003) Isolation and Characterization of *Thermophilic Bacilli* Degrading Cinnamic, 4-Coumaric, and Ferulic Acids. Appl Environ Microbiol 69:1417–1427. https://doi.org/10.1128/AEM.69.3.1417-1427.2003

Silva JCR, Salgado JCS, Vici AC, et al (2020) A novel *Trichoderma reesei* mutant RP698 with enhanced cellulase production. Braz J Microbiol 51:537–545. https://doi.org/10.1007/s42770-019-00167-2

Soy S, Nigam VK, Sharma SR (2021) Enhanced production and biochemical characterization of a thermostable amylase from thermophilic bacterium *Geobacillus icigianus* BITSNS038. J Taibah Univ Sci 15:730–745. https://doi.org/10.1080/16583655.2021.2002549

Sun F, Ou Q, Wang N, et al (2020) Isolation and identification of potassium-solubilizing bacteria from *Mikania micrantha* rhizospheric soil and their effect on M. micrantha plants. Global Ecol Conserv 23:e01141. https://doi.org/10.1016/j.gecco.2020.e01141

Tu Y, Shen J, Peng Z, et al (2023) Biochar-dual oxidant composite particles alleviate the oxidative stress of phenolic acid on tomato seed germination. Antioxidants 12:910. https://doi.org/10.3390/antiox12040910

Wang D, Sun L, Yu H, et al (2023) Whole-genome analysis of the benzoic acid-degrading bacterium *Bacillus halotolerans* B28 to reveal its phytoprobiotic effects. Int Biodeterior Biodegrad 185:105668. https://doi.org/10.1016/j.ibiod.2023.105668

Wang H, Cai X, Xu M, Tian F (2021) Enhanced Biocontrol of Cucumber Fusarium Wilt by Combined Application of New Antagonistic Bacteria *Bacillus amyloliquefaciens* B2 and Phenolic Acid-Degrading *Fungus Pleurotus* ostreatus P5. Front Microbiol 12:700142. https://doi.org/10.3389/fmicb.2021.700142

Wang Z, Tian B, Zhang C, et al (2026) Alleviating continuous cropping obstacles of *Pinellia ternata* and *Pseudostellaria heterophylla*: Remediation of allelochemical phenolic acid-contaminated soils by *Bacillus cereus* WL08 immobilized on coconut shell charcoal. Environ Technol Innovation 43:105033. https://doi.org/10.1016/j.eti.2026.105033

Wu F, Ding Y, Nie Y, et al (2021) Plant metabolomics integrated with transcriptomics and rhizospheric bacterial community indicates the mitigation effects of klebsiella oxytoca P620 on p-hydroxybenzoic acid stress in cucumber. J Hazard Mater 415:125756. https://doi.org/10.1016/j.jhazmat.2021.125756

Xiang W, Wei X, Tang H, et al (2020) Complete Genome Sequence and Biodegradation Characteristics of Benzoic

Acid-Degrading Bacterium *Pseudomonas* sp. SCB32. Biomed Res Int 2020:6146104. https://doi.org/10.1155/2020/6146104

Xu J, Fang J, Wu R, et al (2026) Exploring the genomic features and plant growth-promoting properties of *Enterobacter vonholyi* Y16 isolated from maize rhizosphere. Microbiol Res 305:128437. https://doi.org/10.1016/j.micres.2026.128437

Yang X, Du D, Yang X, et al (2026) Dual-functional *Bacillus amyloliquefaciens* mediates autotoxin degradation and pathogen suppression in monocropped foxtail millet. Biol Fertil Soils 62:441–456. https://doi.org/10.1007/s00374-026-01980-2

Zhang C, Liu S, Guo Q, et al (2024a) *Sphingobium* sp. V4, a bacterium degrading multiple allelochemical phenolic acids. Ann Microbiol 74:5. https://doi.org/10.1186/s13213-024-01750-1

Zhang W, Sun P-Y, Ren R, et al (2025) Application of a Pseudomonas strain mitigates the combined stresses of phenolic acids and salt in soil-grown cucumber. Ecotoxicology and Environmental Safety 303:118822. https://doi.org/10.1016/j.ecoenv.2025.118822

Zhang Y, Wang B, Wang G, et al (2024b) Acidification induce chemical and microbial variation in tea plantation soils and bacterial degradation of the key acidifying phenolic acids. Arch Microbiol 206:239. https://doi.org/10.1007/s00203-024-03858-z

Zhang Z, Gao L, Lu P, et al (2026) Fe@BC/UHP alleviates continuous cropping obstacle by removing benzoic acid in Brassica napus. Sci Hortic 359:114771. https://doi.org/10.1016/j.scienta.2026.114771